Advanced Physical Research
Vol.7, No.2, 2025, pp.222-230
https://doi.org/10.62476/apr.72.222

CHANGING THE ABSORBER LAYER WITH A COMPOUND $FeSi_2$ TO IMPROVE THE EFFICIENCY OF THE SOLAR CELL USING A SIMULATION PROGRAM

H.W. Hamed, M.W. Aziz, N.A. Ahmad*

Department of Physics, College of Education for Women, University of Kirkuk, Iraq

Abstract. This research examines the electrical and optical features of AZO/ZnO/CdS/CIGS solar cell by altering the concentration and thickness of the absorption layer to optimize efficiency. Structural and electrical qualities may be essential in the emerging domains of the optoelectronics industry, where cell efficiency has been achieved. Efficiency = 10.2%, Fill Factor = 68.38%, Short-Circuit Current Density = 34.53 mA/cm^2, Open-Circuit Voltage = 424.2 mV. The cell efficiency was enhanced following the modification of the layer concentration. Copper Indium Gallium Selenide Efficiency = 18.2%, Fill Factor = 81.57%, Short-Circuit Current Density = 32.42 mA/cm^2, Open-Circuit Voltage = 688.3 mV. The efficiency of the solar cell has been seen to grow to 25.7% upon substituting the absorption layer with the combination $FeSi_2$.

Keywords: $FeSi_2$, simulation program, absorber layer.

***Corresponding author:** Noor Abdulwahed Ahmad, Department of Physics, College of Education for Women, University of Kirkuk, Kirkuk, Iraq, e-mail: *noorabdulwahed@uokirkuk.edu.iq*

Received: 5 February 2025; Revised: 17 April 2025; Accepted: 2 May 2025; Published: 24 June 2025.

1 Introduction

The complex physical principles regulating solar cell systems require solar simulation tools, essential for their design and analysis (Soga, 2006). This research seeks to create a theoretical framework that connects material attributes to solar cell functionality and identifies critical physical parameters affecting their performance. The numerical simulation of CIGS thin-film solar cells is conducted utilizing the one-dimensional AFORS-HET program. This program provides critical insights on the impact of parameter variations on the overall performance of solar cells under consistent illumination. In Mickelsen and Chen (1981) sparked interest in CIGS thin-film solar cells, employing an evaporation process to achieve 9.4% efficiency (Mickelsen & Chen, 1981).

The P-type CIGS semiconductor has a blue shift in its characteristics. CIGS-based solar cells possess an ideal potential energy difference and a strong optical absorption coefficient, making them suitable for solar cell applications. When constructed using metal foil or polymer substrates, these cells exhibit flexibility and lightweight characteristics, rendering them ideal for integrated systems. These advantages are accessible across numerous applications. Furthermore, they exhibit greater resistance to radiation compared to solar cells composed of crystalline silicon (Kato, 2017). A notable benefit of CIGS-based solar cells is their diminished material and energy production demands relative to conventional silicon-based solar cells (Powalla et al., 2017).

The power conversion efficiency of Cd-free CIGS solar cells is approximately 23.35%, which is significantly higher than that of traditional thin-film chalcogenide solar cells (Green et al., 2021). Two primary ways for producing CIGS thin-film depositions are selenization and co-

evaporation techniques (Niki et al., 2010). The selenium process is conducted subsequent to the deposition of indium, copper, and gallium metals onto a metalized glass substrate. The co-evaporation method rapidly generates the CIGS layer by thermally evaporating all components under vacuum conditions onto a substrate of metalized glass (Kato, 2017).

The CIGS absorber layer structure with a double-graded band gap, featuring a sulfur-rich layer at the front and a gallium gradient at the rear, mitigates electron-hole recombination at both interfaces, thereby enhancing carrier collection and transport, and improving solar cell efficiency (Khatri et al., 2015, Nagoya et al., 2001). In contrast to traditional first-generation silicon-based solar cells, which are approximately 200 micrometers thick, second-generation thin-film solar cells are significantly thinner, with a customizable thickness ranging from several nanometers to tens of micrometers. Studies have demonstrated that doping concentrations and the absorber thickness, and the hole transport layers influence solar cell efficacy (Bag et al., 2020, Zahoo et al., 2021). This attribute renders thin-film solar cells lighter and more versatile, while minimizing material usage (Efaz et al., 2021).

The semiconductor iron silicon dioxide ($FeSi_2$) has an extraordinarily high coefficient of optical absorption (alpha greater than 10^5 cm^{-1}), is expected to be an ideal material for thin-film solar cells (Fukuzawa et al., 2006). The optical absorption coefficient of beta-$FeSi_2$ is around 10^5 cm^{-1}, corresponding to photon energies above 1 eV. At a photon energy of 6.26 eV, the value reaches a maximum of 2.67 times 10^5 cm^{-1}. A 1 micrometer thick beta-$FeSi_2$ film absorbs practically all sunlight (Chen et al., 2014). Therefore, $FeSi_2$ is theoretically a new photoelectric element with an efficiency of 16-23 percent (Waleed et al., 2022).

AFORS-HET is a simulation program designed to manage both homojunction and heterojunction semiconductors. It can replicate interface and bulk recombination by including flaws into semiconductor layers. The application provides multiple transport models, including thermionic emission and drift-diffusion, to illustrate the flow of holes and electrons inside semiconductor layers, utilizing functions such as exponential, linear, Gaussian, or error functions to represent semiconductor features (Munef et al., 2022). Furthermore, the connections of the front and rear solar cells can be represented as metal/insulator/semiconductor, Schottky, or insulator interfaces, providing diverse experimental design options (Stangl et al., 2010; 2012).

The primary objective of this study is to utilize 1D-AFORS-HET simulations to evaluate parameters for enhancing CIGS solar cells. We commenced by analyzing how the performance is affected by the thickness of the absorber layer of CIGS photovoltaic cells. The simulation is beneficial for assessing and forecasting device results and the effects of parameters without the need to manufacture the device. To guarantee reliable outcomes, we assessed the simulation against experimental data from Jiang Liu and associates (Liu et al., 2013), enhancing solar cell performance by appropriately adjusting parameters.

2 Solar Cell Simulation

Semiconductor materials display changeable properties, especially in thin film solar cells, where faults can migrate inside device layers as processing temperatures rise during production. The contact between semiconductor layers considerably affects the properties of certain solar cells (Stangl et al., 2012). In the following electrical simulation phase, the generation rate derived from the optical simulation is utilized as input. Electrical modeling in semiconductor layers calculates electric potential and carrier densities under various boundary conditions. Carrier densities and electric potential can be utilized to predict further internal solar cell properties, including phase shifts, currents, band diagrams, and recombination rates (Stangl et al., 2012).

Optical and electrical simulations of solar cells can be conducted independently using methods such as FDTD (Abdulrahman et al., 2013) and DEVICE simulation (Arjmand et al., 2013). The generation rate in semiconductor layers, defined as the quantity of the amount of electrons and holes produced per unit volume per second at a given location and time can be determined

by optical modeling as a result of light absorption.

Many aspects can be incorporated into an optical model for simulation, including coherent superposition of propagating light, internal surface light scattering, and exterior and internal reflections. By addressing the steady-state equations of electrons and holes, as well as Poisson equation, the electric potential and carrier densities can be determined. Contemporary simulations originate from Gummel 1964 concept for the numerical modeling of semiconductor devices. Shockley-Read-Hall (SRH) recombination, Auger recombination (non-radiative recombination), and radiative recombination are effects that may be incorporated into simulations, contingent upon the chosen recombination model (Stangl et al., 2012).

3 Generation

The generation rate of the optical super-band gap $G_n = G_p$ (when $h_c$lambda/E_g) when photons illuminate heterostructure semiconductor layers with flux input (phi(lambda)), can be ascertained through various approaches. Initially, the Beer-Lambert law is utilized, assigning a specific absorption coefficient, alpha, to each layer. Secondly, dielectric properties (n, k) are attributed to each layer, and variable reflections (coherent/incoherent) within the layers are accounted for. Finally, SRH recombination, characterized by the assignment of optical emission coefficients, can be utilized to calculate the rate from defects to the valence and/or conduction band when h_c lambda/E_g.

$e_n{}^0$(E), $e_p{}^0$(E) not equal to 0 for the defect state (Stangl et al., 2012):

$$e_n^0(E,x) = \sigma_n^0 N_c \phi(\lambda,x)\vartheta(E_c - E - h_c/\lambda) \tag{1}$$

$$e_p^0(E,x) = \sigma_p^0 N_V \phi(\lambda,x)\vartheta(E - E_V - h_c/\lambda) \tag{2}$$

Where: sigma$_n{}^0$: capture cross sections to record holes and electrons, N_c, N_V: band density for valence and conduction, E_C, E_V: band energy for valence and conduction.

This approach enables thorough modeling of optical and recombination processes in semiconductor layers under illumination, essential for comprehending and enhancing solar cell performance. SRH recombination during the transition from the conduction band to the valence band, Auger recombination, radiative recombination, as well as defect states within the semiconductor band gap (Stangl et al., 2012):

$$R_{n,p}(x,t) = R_{n,p}^{direct}(x,t) + R_{n,p}^{SRH} \tag{3}$$

The direct band-to-band recombination rate r^{BB} and Auger rate constants $r_n{}^A$, $r_p{}^A$ must be specified:

$$R_{n,p}^{direct}(x,t) = R_{n,p}^{direct}(x) + \tilde{R}_{n,p}^{direct}(x)e^{iwt} \tag{4}$$

A random distribution of defect states is required within the semiconductor band gap to calculate SRH recombination. Furthermore, the dispersion of energy N_t(E) of each mistake in the semiconductor band gap and the corresponding capture coefficients needs to be defined as $C_{n,p} = V_{n,p}$sigma$_{n,p}$ for electrons and holes, where $V_{n,p}$ represents thermal velocity and sigma$_{n,p}$ signifies capture cross-section:

$$R_{n,p}^{SRH}(x,t) = R_{n,p}^{SRH}(x) + \tilde{R}_{n,p}^{srh}(x)e^{iwt} \tag{5}$$

The function for distribution f_t(E,x,t) is derived from the SRH theory, describing the occupation of defect states (Stangl et al., 2010):

$$f_t(E,x,t) = f_t(E,x) + \tilde{f}_t(E,x)e^{iwt} \tag{6}$$

This approach enables thorough modeling of optical and recombination processes in semiconductor layers under illumination, essential for comprehending and enhancing solar cell performance.

4 Solar Cell Configuration

Cellular architecture Figure 1 depicts AZO/ZnO/CdS/CIGS. A cadmium sulfide layer was utilized as a trapping layer, copper indium gallium selenide served as the absorption layer, and zinc oxide functioned as the transparent conductive oxide. The measured temperature was 300 K under standard light of 1.5G AM. The thermal velocity of the electrons was 10^7 cm for each layer, and the work function for the back contact was 5.2 eV.

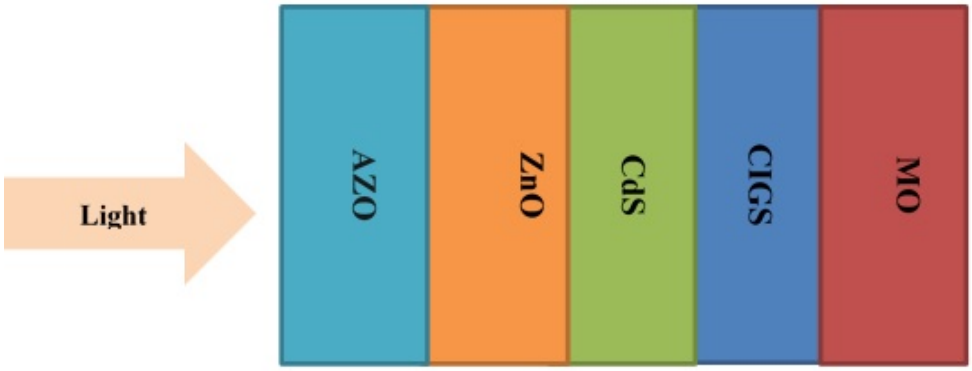

Figure 1: Solar Cell Structure AZO/ZnO/CdS/CIGS

Table 1 shows the input parameters for the simulation program.

Table 1: Input parameters for Simulation program

$FeSi_2$	**CIGS**	**CdS**	**ZnO**	**AZO**	**Symbol**	**Parameters**
–	100	50	100	–	d (nm)	Thickness
30	13.6	10	9	9	dk	Dielectric constant
4.16	4.4	4.2	4	4.5	X (eV)	Electron affinity
0.88	1.3	2.4	3.3	3.3	Eg (eV)	Band gap
1.7E18	2.2E18	1.3E18	3.7E18	3E18	Nc (cm-3)	Density of state CB
1.7E18	1.5E19	9.1E19	1.8E19	1.7E18	Nv (cm-3)	Density of state VB
400	100	72	100	100	mu-n (cm2/Vs)	Electron mobility
20	25	20	25	25	mu-p (cm2/Vs)	Hole mobility
2E16	5E16	0	0	0	Na (cm-3)	Acceptor conc.
0	0	1E20	1E20	1E20	Nd (cm-3)	Donor conc.
1E7	1E7	1E7	1E7	1E7	Vth (cm/s)	Thermal velocity
2.328	2.328	2.328	2.328	2.328	rho (g/cm3)	Layer density
1.64	AFORS-HET	AFORS-HET	AFORS-HET	AFORS-HET	n	Refractive index
2.55	–	–	–	–	k	Extinction coeff.

5 Results and Discussion

5.1 Cell Structural Optimization Results

Figure 2 illustrates the voltage characteristics of the cell (AZO/ZnO/CdS/CIGS). Prior to enhancement, it exhibits linear current and voltage characteristics attributed to the energy gap absorption of the CIGS layer (Eg = 1.3 eV), signifying an ohmic connection with a junction resistance of 4 ohms, as depicted below in a non-linear manner.

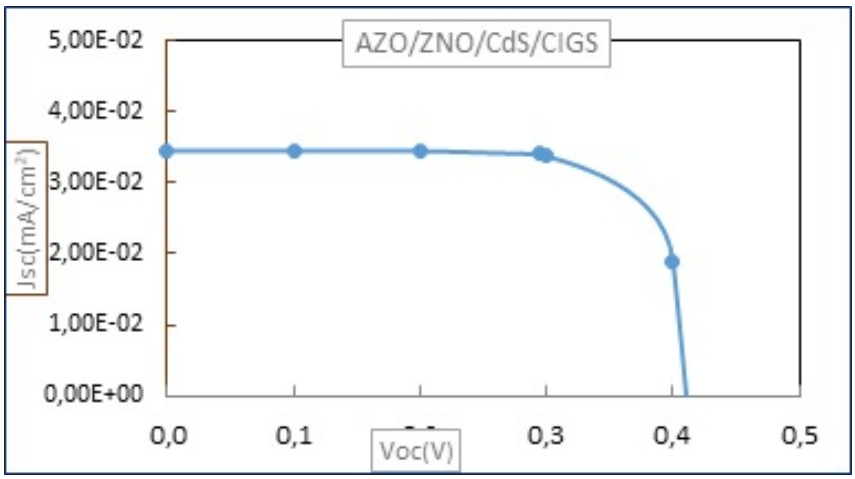

Figure 2: Current-Voltage characteristic

Table 2: The cell results

CELL	**Jsc** (mA/cm^2)	**Voc (V)**	**FF (%)**	**Eff (%)**
AZO/ZnO/CdS/CIGS	34.53	424.2	68.38	10.02

5.2 Effect of Changing CIGS Concentration within the Absorption Layer

Influence of differing CIGS concentrations in the absorber layer on the band gap of pure CIGS (1.3 eV) in solar cells. All parameters for the remaining layers have been configured with the alteration in concentration from (5E10 - 5E16) cm^{-3}. Figure 3 illustrates an increase in Voc, efficiency, and fill factor as the concentration of CIGS in the absorber layer varies, affecting the fill factor, efficiency response, open circuit voltage, and short circuit current. The photovoltaic under an acceptor density of 10^{15} cm^{-3}, the CIGS absorber performance parameters are practically identical. The device outputs are altered at elevated concentrations (Rahman et al., 2022). Nonetheless, attaining such elevated doping levels in absorber materials experimentally is quite challenging. Consequently, to mitigate complexity and decrease costs (Ali et al., 2023).

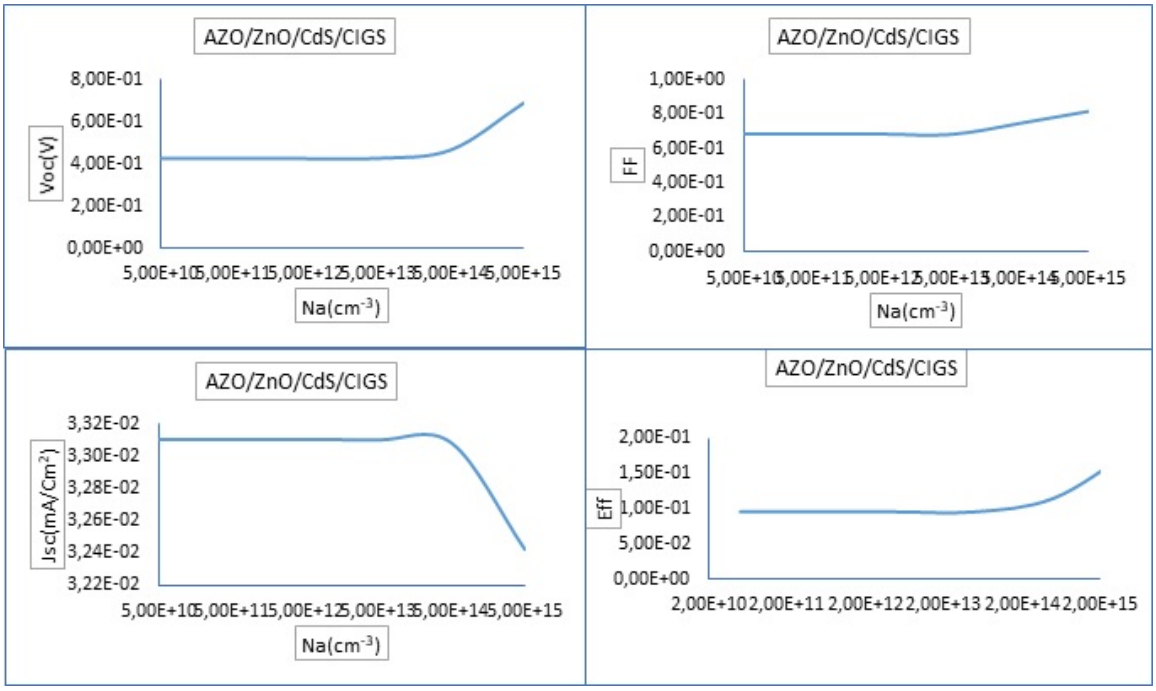

Figure 3: Effect of changing CIGS concentration inside the layer of absorbers

5.3 Influence of Absorber Layer Thickness on Solar Cell Efficiency

The percentage of incident solar photons absorbed by CIGS layers grows in direct proportion to their thickness, resulting in enhanced efficiency (eta) (Rahman et al., 2022). The simulation findings indicate that the open circuit voltage, fill factor, short circuit current, and efficiency all increase as the thickness of the CIGS absorber layer varies from 100 nm to 1 micrometer. When high-energy photons strike the front face of the solar cell, they generate electron-hole recombination by entering the absorber layer, occurring at the device rear face. Figures 4 and 5 illustrate the effects of different CIGS layer thicknesses on Voc, Jsc, FF, efficiency, and energy output of the solar cell.

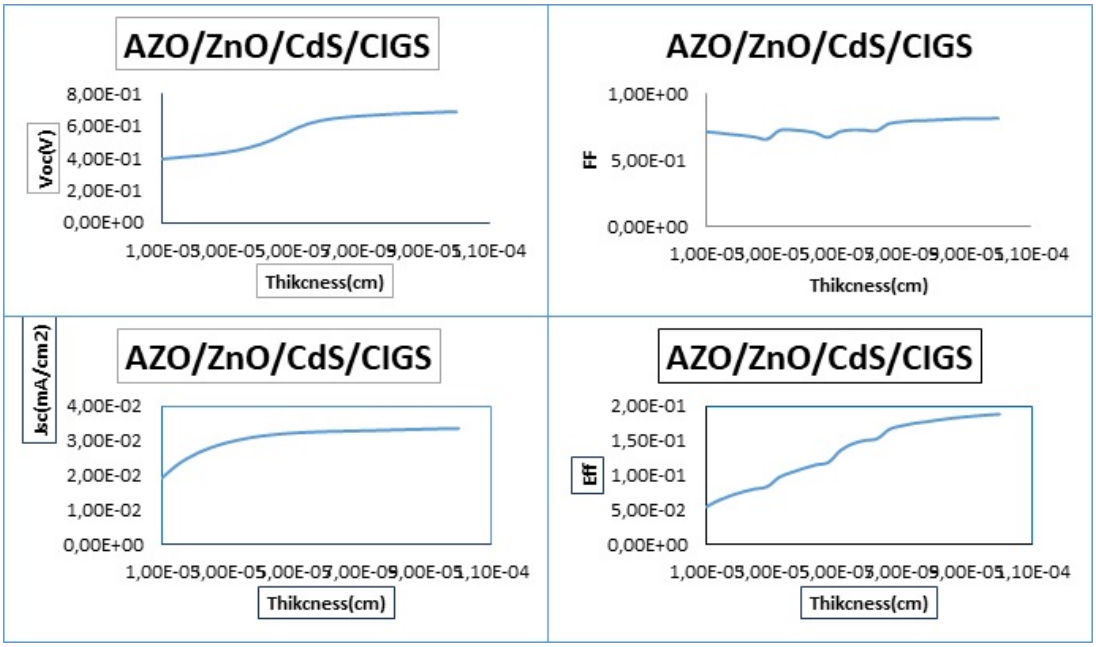

Figure 4: Effect of CIGS layer thickness variation on (a) Voc, (b) Jsc, (c) FF, (d) Eff

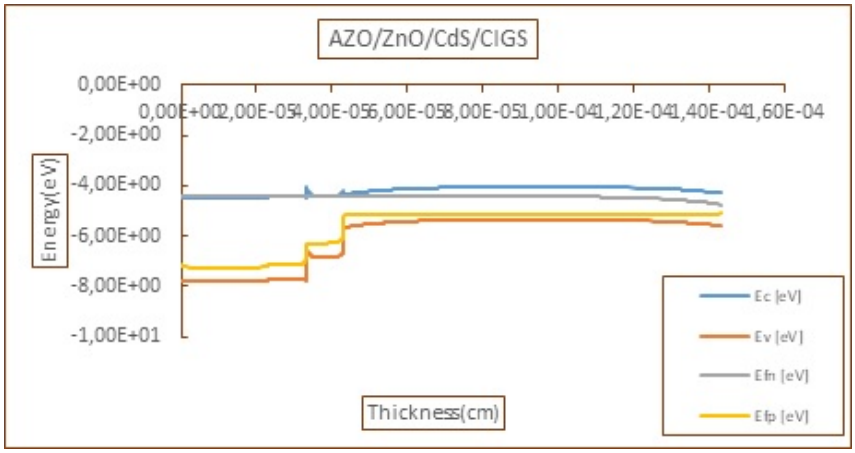

Figure 5: Effect of changing the thickness on energy

5.4 The Results of Using a FeSi2 Layer Instead of a CIGS Absorber Layer

Substituting the CIGS layer with a $FeSi_2$ layer and observing the concentration variation in order to make the solar cell work better. The $FeSi_2$ layer exhibited a band gap of 0.88 eV, while the pure CIGS absorber layer displayed a band gap of 1.3 eV. We maintained all parameters of the other layers while replacing the CIGS layer with the $FeSi_2$ layer. The short circuit current, open circuit voltage, fill factor, and efficiency response are all influenced when the CIGS absorber layer is replaced with the $FeSi_2$ layer, as illustrated in Figure 6. It is also evident that FF, Eff, Voc, and Jsc all increase when the absorber layer is altered.

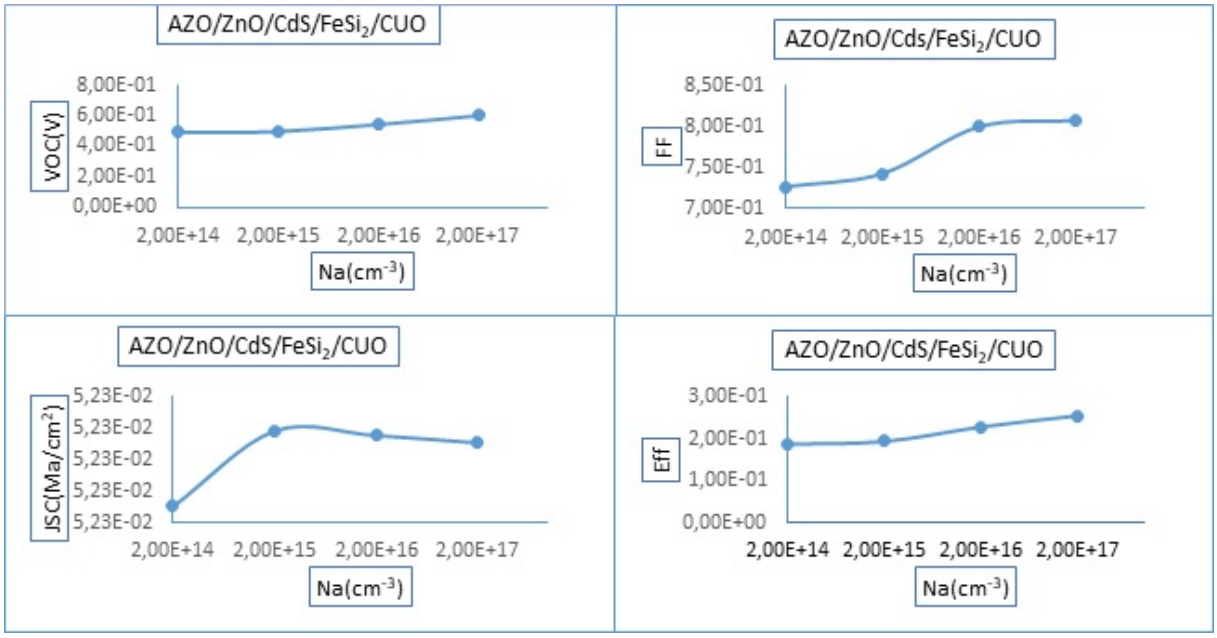

Figure 6: Replacing the CIGS absorber layer with the $FeSi_2$ layer

6 Conclusion

The impact of the material thickness on the CIGS insulation layer, concentration, and substitution with $FeSi_2$ layer on solar cell efficiency was analyzed utilizing AFORS-HET software. The ideal parameters to the layer that acts as an absorber were subsequently determined. The substitution of the CIGS absorber layer with a $FeSi_2$ layer influences the efficacy of the photo-

voltaic cell. We successfully extracted the enhancement of the $FeSi_2$ cell structure. The efficiency demonstrated an enhancement of Eff = 25.7%, Voc = 688.3 mV, FF = 81.57%, Jsc = 32.42 mA/cm^2.

7 Acknowledgement

The authors would like to thank the University of Kirkuk for providing the computational resources necessary for this research. The work is supported by the Department of Physics, College of Education for Women.

References

Abdulrahman, R.B., Alagoz, A.S., & Karabacak, T. (2013). Enhanced light trapping in periodic aluminum nanorod arrays as cavity resonator. *MRS Online Proceedings Library, 1566*(1), 345-350.

Ali, M.H., Islam, A.S., Haque, M.D., Rahman, M.F., Hossain, M.K., Sultana, N., & Islam, A.T. (2023). Numerical analysis of FeSi2 based solar cell with PEDOT: PSS hole transport layer. *Materials Today Communications,* 34, 105387.

Arjmand, A., McGuire, D. (2013). Complete optoelectronic simulation of patterned silicon solar cells. *13th International Conference on Numerical Simulation of Optoelectronic Devices*, NUSOD 2013, 13-14.

Bag, A., Radhakrishnan, R., Nekovei, R., & Jeyakumar, R. (2020). Effect of absorber layer, hole transport layer thicknesses, and its doping density on the performance of perovskite solar cells by device simulation. *Solar Energy,* 196, 177-182.

Chen, F.X., Xu, W.Y., & Wang, J.F. (2014). beta-FeSi2/p-Si heterojunction solar cells simulation by AFORS-HET. *Journal of Optoelectronics and Advanced Materials, 16*(3-4), 494-498.

Efaz, E.T., Rhaman, M.M., Al Imam, S., Bashar, K.L., Kabir, F., Mourtaza, M.E., Sakib, S.N., & Mozahid, F.A. (2021). A review of primary technologies of thin-film solar cells. *Engineering Research Express, 3*(3), 032353.

Fukuzawa, Y., Ootsuka, T., Otogawa, N., et al. (2006). Photonics for Solar Energy Systems, 6197, 61970E.

Green, M., Dunlop, E., Hohl-Ebinger, J., Yoshita, M., Kopidakis, N., & Hao, X. (2021). Solar cell efficiency tables (version 57). *Progress in photovoltaics: research and applications, 29*(1), 3-15.

Kato, T. (2017). Cu (In, Ga)(Se, S)2 solar cell research in Solar Frontier: Progress and current status. *Japanese Journal of Applied Physics, 56*(4S), 04CA02.

Khatri, C., Chapman, S.J., Glasbey, J., Kelly, M., Nepogodiev, D., Bhangu, A., & STARSurg Committee. (2015). Social media and internet driven study recruitment: evaluating a new model for promoting collaborator engagement and participation. *PloS one, 10*(3), e0118899.

Liu, J., Zhuang, D., Luan, H., Cao, M., Xie, M., & Li, X. (2013). Preparation of Cu(In,Ga)Se2 thin film by sputtering from Cu(In,Ga)Se2 quaternary target. *Progress in Natural Science: Materials International, 23*(2), 133-138.

Mickelsen, R.A., Chen, W.S. (1981). Development of a 9.4 percent efficient thin-film CuInSe2/CdS solar cell. *15th Photovoltaic Specialists Conference*, 800-804.

Munef, R.A., Ameen, M.M., Rosure, B.A., Waleed, H., & Ghelab, A.M. (2022). Optimizing the Parameters of CIGS Solar Cells Using One-Dimension AFORS-HET Program. *NeuroQuantology, 20*(2), 69.

Nagoya, Y., Kushiya, K., Tachiyuki, M., and Yamase, O. (2001). Role of incorporated sulfur into the surface of Cu (InGa) Se2 thin-film absorber. Solar Energy Materials and Solar Cells, 67(1-4), 247-253.

Niki, S., Contreras, M., Repins, I., Powalla, M., Kushiya, K., Ishizuka, S., & Matsubara, K. (2010). CIGS absorbers and processes. *Progress in Photovoltaics: Research and Applications, 18*(6), 453-466.

Powalla, M., Paetel, S., Hariskos, D., Wuerz, R., Kessler, F., Lechner, P., & Friedlmeier, T.M. (2017). Advances in cost-efficient thin-film photovoltaics based on Cu (In, Ga) Se2. *Engineering, 3*(4), 445-451.

Rahman, M.F., Moon, M.M.A., Hossain, M.K., Ali, M.H., Haque, M.D., Kuddus, A., & Ismail, A.B.M. (2022). Concurrent investigation of antimony chalcogenide (Sb2Se3 and Sb2S3)-based solar cells with a potential WS2 electron transport layer. *Heliyon, 8*(12), e12034.

Rahman, M.F., Habib, M.J.A., Ali, M.H., Rubel, M.H.K., Islam, M.R., Md Ismail, A.B., & Hossain, M.K. (2022). Design and numerical investigation of cadmium telluride (CdTe) and iron silicide (FeSi2) based double absorber solar cells to enhance power conversion efficiency. *AIP Advances, 12*(10), e105201.

Soga, T. (Ed.). (2006). *Nanostructured materials for solar energy conversion*. Elsevier.

Stangl, R., Leendertz, C., & Haschke, J. (2010). Numerical simulation of solar cells and solar cell characterization methods: the open-source on demand program AFORS-HET. *Solar Energy,* 14, 319-352.

Stangl, R., Leendertz, C. (2012). General Principles of Solar Cell Simulation and Introduction to AFORS-HET. In *Physics and Technology of Amorphous-Crystalline Heterostructure Silicon Solar Cells*, Springer, Berlin, Heidelberg, 445-458.

Waleed, H., Munef, R. A., & Saleh, A.N. (2022). Simulation and improvement of FeSi2/Si solar cell by AFORS-HET software. *AIP Conference Proceedings,* Vol. 2398, No. 1.

Zahoo, R.K., Saleh, A.N. (2021). Effect of Carrier Concentration and Thickness of Absorber Layer on Performance CBTS Solar Cell. *Turkish Journal of Computer and Mathematics Education, 12*(10), 5056-5064.